ELSEVIER

Sensors and Actuators B 76 (2001) 582–593

SENSORS AND ACTUATORS B CHEMICAL

www.elsevier.nl/locate/sensorb

A novel pH sensitive ISFET with on chip temperature sensing using CMOS standard process

Yuan-Lung Chin[a], Jung-Chuan Chou[b,*], Tai-Ping Sun[c], Wen-Yaw Chung[a], Shen-Kan Hsiung[a]

[a]*Institute of Electronic Engineering, Chung Yuan Christian University, Chung-Li 320, Taiwan, ROC*

[b]*Institute of Electronic and Information Engineering, National Yunlin University of Science and Technology, Touliu, Yunlin 640, Taiwan, ROC*

[c]*Department of Electrical Engineering, National Chi Nan University, Nantou 545, Taiwan, ROC*

Abstract

A monolithic chip processing method is reported, which includes the ion sensitive field effect transistor (ISFET) of the pH sensor, p–n diode of temperature sensor and readout circuit using 0.5 μm double poly double metal (DPDM) standard CMOS product with UMC IC foundry company. We have designed a planar diffused silicon diode on a n-channel pH sensitive ISFET sensor to act as a temperature sensor for on-chip temperature measurement and compensation. Furthermore, the device integrated the dual sensors and readout circuit has the potential advantages of achieving, both the pH and temperature value display, with this process, ISFET's temperature coefficient can be minimized.

Keywords: Ion-sensitive field effect transistor (ISFET); pH sensor; p–n Diode; DPDM; CMOS

1. Introduction

ISFET pH sensors are being used increasingly for a variety of purposes in the chemical, medicine and biological industries, as well as various fields of basic research. Apart form their small size, robustness, low power consumption and simplicity in fabrication, ISFETs have a distinct advantage over conventional pH measuring systems [1]. Investigations have demonstrated that ISFETs have a large thermal instability, which leads to inaccuracy in measurements. It is often necessary for ISFETs to be used under thermostatic conditions to ensure the necessary accuracy. Since this is not convenient for many applications, it is important to investigate the thermal behavior of ISFETs to determine effective methods to improve their stability.

In the previous papers published by Gui et al. [2] on ISFET temperature pair compensation, the ISFET and MOSFET differential pair configuration with a low doping concentration can reduce the temperature coefficient. Aw and Cheung [3] reported that ISFET exists the athermal point, which is empirically determined to be at a drain current of 50 μA, and combine dual sensor for pH and temperature.

In this study, we report a method for ISFET temperature compensation. A summation circuit was used to combine an ISFET and a p–n temperature sensor diode as shown in Fig. 1. Using the p–n diode negative temperature coefficient and the ISFET positive temperature coefficient together, the two sensors can reduce the temperature characteristics of the ISFET. In order to simplify the sensor fabrication into one chip, the ISFET, p–n diode and readout circuit were produced using a CMOS standard IC process.

The ISFET temperature characteristics (TC) are investigated and analyzed in Section 2. According to the TC, methods to reduce the ISFET TC are developed. Section 3 presents the ISFET and p–n diode sensors produced using the standard CMOS process. The readout circuit for the ISFET temperature compensation is discussed in Section 4. The experimental results and discussion are reported in Section 5 followed by the conclusion.

2. Temperature characteristics of the ISFET

To derive a temperature model of the ISFET, the following temperature coefficients were considered: reference electrode, test solution, pH sensitive film/electrolyte interface and the field effect transistor.

2.1. Temperature coefficient of the reference electrode (T_R)

The reference electrode used to measure the temperature characteristics was the Ag/AgCl electrode with a filling of

* Corresponding author. Tel.: +886-5-5342601/ext. 2500; fax: +886-5-5312029.
E-mail address: choujc@pine.yuntech.edu.tw (J.-C. Chou).

0925-4005/01/$ – see front matter
PII: S0925-4005(01)00639-6

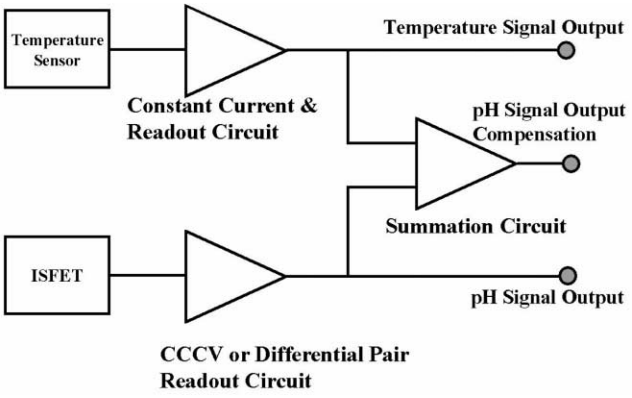

Fig. 1. Block diagram of the ISFET temperature compensation.

3.5 M KCl, saturated with AgCl. The potential of this type of reference electrode is as following [4]:

$$E_{\mathrm{Ref}}(T) = E_{\mathrm{ABS}}\left(\frac{\mathrm{H}^+}{\mathrm{H}_2}\right) + E_{\mathrm{Ref}}\left(\frac{\mathrm{Ag}}{\mathrm{AgCl}}\right) + \left(\frac{\mathrm{d}E_{\mathrm{Ref}}}{\mathrm{d}T}\right)(T - 298.16) \quad (1)$$

where $E_{\mathrm{ABS}}(\mathrm{H}^+/\mathrm{H}_2)$ is the normalized hydrogen potential.

In the above equation, the temperature coefficient term is applied when the hydrogen electrode is maintained at 25°C. According to the experimental results [5], the temperature coefficient of the $\mathrm{d}E_{\mathrm{Ref}}/\mathrm{d}T$ is equal to 0.14 mV/°C for an Ag/AgCl electrode. The value of $E_{\mathrm{ABS}}(\mathrm{H}^+/\mathrm{H}_2)$ is a temperature-independent. Hansen and Kolb [7] and Bousse reported values of 4.73, 4.7 and 4.74 V, respectively [6–8]. The relative potential of the reference electrode E_{Ref}(Ag/AgCl) is a constant 0.205 V. The above equation can be written as following:

$$E_{\mathrm{Ref}}(T) = 4.7 + 0.205 + 1.4 \times 10^{-4}(T - 298.16) = 4.905 + 1.4 \times 10^{-4}(T - 298.16) \quad (2)$$

The liquid-junction potential for the Ag/AgCl electrode with a 3.5 M KCl filling solution is typically quite small. For a typical liquid-junction potential of 3 mV, the value of this temperature coefficient is 10 μV/K.

2.2. Test solution (T_S)

Since the pH value of an electrolyte solution is a negative logarithmic form of the H^+ activity in the electrolyte, which is a function of temperature. This variation in the pH value in an electrolyte solution affects the measured results. The pH values and the temperature coefficients used in this study are listed in Table 1.

2.3. pH sensitive film/electrolyte interface (T_I)

The potential between pH sensitive film/electrolyte interface is also temperature-dependent. This phenomenon can be explained using a site-binding model [10,11] as shown in Eq. (3).

Table 1
Temperature coefficients for the different buffer solutions [9]

Temperature coefficients (°C)	pH 2	pH 4	pH 6	pH 8	pH 10
25	2	4	6	8	10
35	2.03	4.03	6	7.97	9.94
45	2.06	4.12	6.01	7.92	9.87
55	2.08	4.17	6.02	7.86	9.84

$$2.303(\mathrm{pH}_{\mathrm{PZC}} - \mathrm{pH}) = \frac{q\phi_0}{KT} + \sinh^{-1}\left(\frac{q\Psi_0}{kT\beta}\right) \quad (3)$$

where

$$\beta = \frac{2q^2 N_{\mathrm{s}}\sqrt{K_{\mathrm{b}}/K_{\mathrm{a}}}}{KTC_{\mathrm{DL}}} \quad (4)$$

In this model the parameters such as K_{a}, K_{b}, N_{s}, and C_{DL} are temperature-dependent, where K_{a}, K_{b} are dissociation constants for potential determining ion and counter-ion surface reactions as shown in the Eqs. (5)–(8).

$$\mathrm{MOH_2}^+ \overset{K_{\mathrm{a}}}{\leftrightarrow} \mathrm{MOH} + \mathrm{H_s}^+ \quad (5)$$

$$K_{\mathrm{a}} = \frac{[\mathrm{MOH}][\mathrm{H}^+]_{\mathrm{b}}\exp(-q\Psi_0)/kT}{[\mathrm{MOH_2}^+]} \quad (6)$$

$$\mathrm{MOH} \overset{K_{\mathrm{b}}}{\leftrightarrow} \mathrm{MO}^- + \mathrm{H_s}^+ \quad (7)$$

$$K_{\mathrm{b}} = \frac{[\mathrm{MO}^-][\mathrm{H}^+]_{\mathrm{b}}\exp(-q\Psi_0)/kT}{[\mathrm{MOH}]} \quad (8)$$

That the total number of sites per unit area is as following:

$$N_{\mathrm{s}} = [\mathrm{MO}^-] + [\mathrm{MOH}] + [\mathrm{MOH_2}^+] \quad (9)$$

The double layer capacitance is as following:

$$C_{\mathrm{DL}}^{-1} = \left[\frac{2kT}{q}\right](8kT\varepsilon_{\mathrm{r}}\varepsilon_0 C)^{-1/2} + C_{\mathrm{h}}^{-1} \quad (10)$$

Tang [12] derived the temperature coefficient of the pH sensitivity film/electrolyte interface. In order to derive this complexity factor, he made some assumptions as to which N_{s} and C_{DL} are temperature-independent. From his results, the temperature coefficient of the pH sensitive film/electrolyte interface is not only temperature-dependent but will also change when different test solutions are used. Using his derived equations, a series of simulation results were derived from pH sensitive membrane/electrolyte interfaces using different values of K_{a}, K_{b} and N_{s} under different temperatures. Fig. 2 shows the temperature coefficient of the interface potential versus different N_{s}. Fig. 3 shows the temperature coefficient of the interface potential versus different K_{a}. Fig. 4 shows the temperature coefficient of the interface potential versus different K_{b}. From these results, the temperature coefficient of the pH sensitive

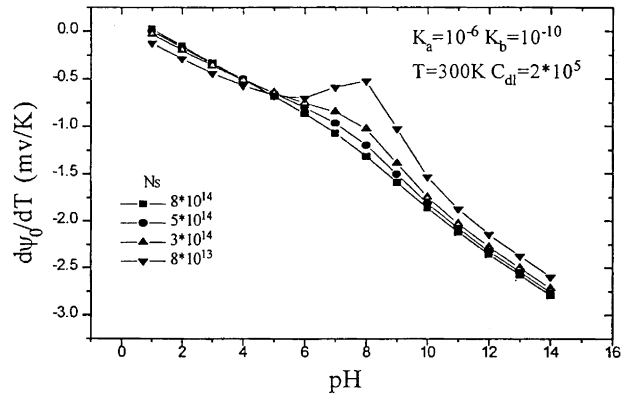

Fig. 2. Simulation of temperature coefficient of interface potential vs. different N_s.

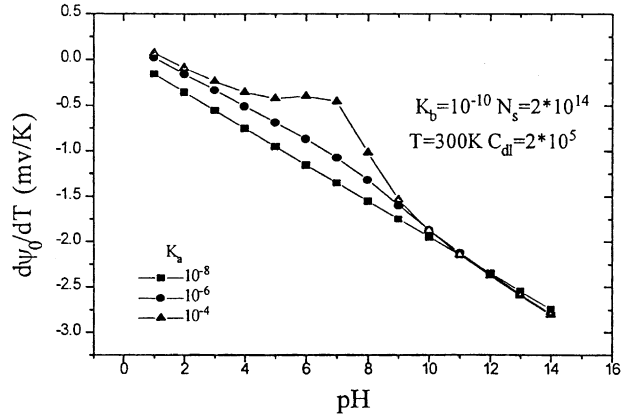

Fig. 3. Simulation of temperature coefficient of interface potential vs. different K_a.

membrane/electrolyte interface is not only a temperature-dependent but also will change when different test solutions are used. These curves become linear and agree with the Nernst equation, when the K_a is small, K_b is large or N_s is large.

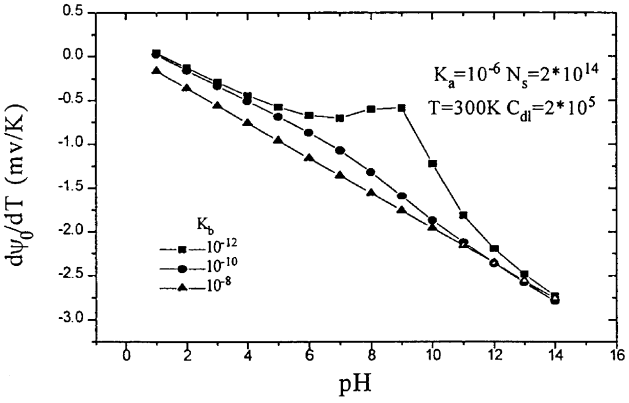

Fig. 4. Simulation of temperature coefficient of interface potential vs. different K_b.

2.4. Field effect transistor (T_F)

Because that the ISFET is a chemical sensor based on the MOSFET, the ISFET temperature characteristics are similar to a conventional MOSFET [13]. The variations of the threshold voltage in an ISFET are usually determined by a feedback circuit, in which the gate-to-source voltage is adjusted to keep the constant drain current, while the source-to-drain voltage remains to be fixed. The current equation of the field effect transistor in the linear region is given by Eq. (11)

$$I_{DS} = \beta\left(V_{GS} - V_T - \tfrac{1}{2}V_{DS}\right)V_{DS} \tag{11}$$

Assuming that the source and the substrate are grounded, where the parameter β in Eq. (11) which is the product of the carried mobility in the silicon surface, the width over length ratio of the transistor, and the insulator capacitance. Taking the temperature derivative of this equation with V_{DS} constant, we obtain the Eq. (12).

$$\frac{\partial V_G}{\partial T} = \frac{\partial V_T}{\partial T} + \frac{I_D}{V_D}\frac{\partial}{\partial T}(\beta^{-1}) \tag{12}$$

The last term in this equation can be found by measuring the dependence of $\partial V_G/\partial T$ on I_D. By taking calculate and measurement at various drain-to-source currents and extrapolating to I_D that is to determine $\partial V_G/\partial T$ be equal zero. And I_D point as the isothermal point [14,15].

Following the above results, the current equation, Eq. (11), in which the MOS of aspect *W/L* is equal to 600 μm/20 μm, when the temperatures are between 30 and 130°C, step 20°C. These results are shown in Fig. 5.

According to above results we can see that the isothermal point at which the threshold voltage and mobility affects the MOS at different temperatures. The various isothermal points with the different aspect ratios *W/L* are shown in Fig. 6.

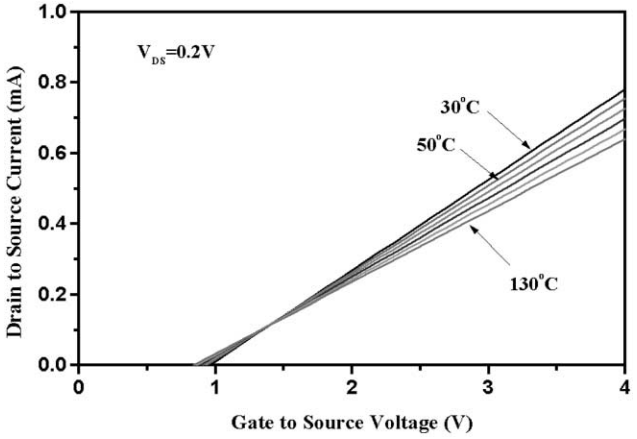

Fig. 5. Calculated data of threshold voltage and mobility in different temperature. Curves of the drain-to-source current vs. gate-to-source voltage under different temperatures by calculation.

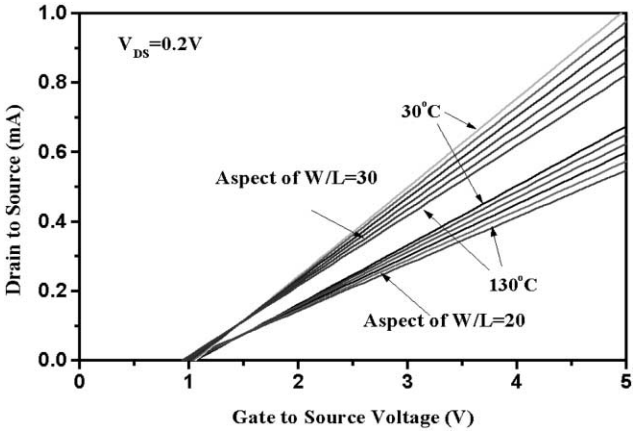

Fig. 6. Curves of the drain-to-source current vs. gate-to-source voltage under different temperatures, where the aspect ratios of *W/L* are 20, 30, respectively.

Fig. 7 shows the experiment for the MOS drain-to-source current versus gate-to-source voltage, the ambient temperatures are 25, 30, 50, 70, 100 and 130°C, respectively. The aspect ratio of the MOS is 600 μm/20 μm. The drain-to-source voltage is 0.2 V, the results compare with above calculation is very similar.

From the above investigation and analysis, the temperature coefficients T_T of the entire ISFET system can be written as

$$T_T = T_R + T_S + T_I + T_F \tag{13}$$

In these items, the T_R and T_S almost are constant. The T_F and the T_I should be investigated according to the drain-to-source current equation of the linear region.

$$I_D = \beta V_{DS}(V_o - E_{Ref} + \Psi_0 - V_T) \tag{14}$$

where the Ψ_0, V_T are dependent on the T_I, T_F, respectively.

The above equation is made differential by the temperature (T), we can get the Eq. (15)

$$\frac{\partial V_o}{\partial T} = \frac{I_D}{V_{DS}}\frac{\partial}{\partial T}(\beta^{-1}) + \frac{\partial E_{Ref}}{\partial T} - \frac{\partial \Psi_0}{\partial T} + \frac{\partial V_T}{\partial T} \tag{15}$$

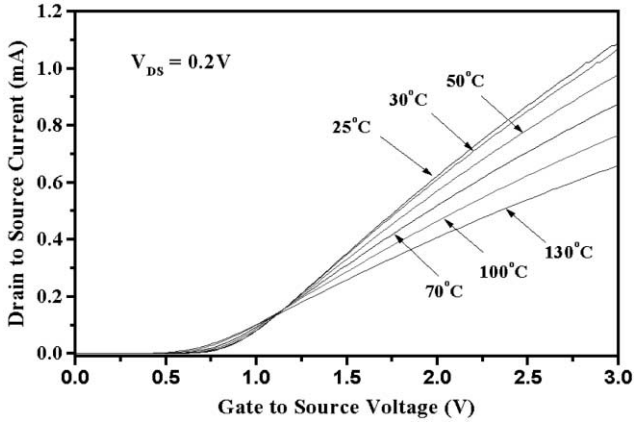

Fig. 7. Curves of the drain-to-source current vs. gate-to-source voltage under different temperatures by experiment.

where the V_o is output voltage of the ISFET. Following Eq. (15), we can determine the output voltage of the ISFET. The term for $(\partial E_{Ref}/\partial T - \partial \Psi_0/\partial T + \partial V_T/\partial T)$ is a negative constant, when a current of (I_D/V_{DS}) $\partial/\partial T(\beta^{-1})$ is fixed, a zero temperature coefficient, called the isothermal point can be acquired. The $\partial E_{Ref}/\partial T$ (T_R) and $-\partial \Psi_0/\partial T$ (T_I) terms, which are dependent on pH value, and produce different isothermal points using different pH buffer solutions. The isothermal point method can be used at a narrow range of pH value, for example the human blood (the pH value between 6.8 and 7.6). If a broad range of pH values is used, then the method of temperature compensate appropriately for a differential pair of ISFET and MOSFET is necessary. In the above section, we noted that both the MOSFET and ISFET have relatively large dV_T/dT (T_F), which needs to be compensated by an ISFET and MOSFET differential pair. The circuit is shown in Fig. 15. The ISFET temperature parameters as reference electrode (T_R) and pH sensitive film/electrolyte interface (T_I) do not have revision. To resolve this question, we used the p–n diode to combine the summation circuit to produce an independent temperature of the ISFET. The temperature coefficients of T_R and T_I have positive values, which are dependent on the temperature as in the above investigation. A silicon diode with stable temperature characteristic has a negative value, which is dependent on the temperature that can be combined with the ISFET and a readout circuit to reduce the T_R, T_I effect and get the precise ISFET pH value and reduce the temperature coefficient [16–20].

3. Integrated sensor design

To produce an ISFET using a CMOS compatible process with no required extra mask. An extended [21] gate SnO_2/Al multi-layer electrodes sensor that consisting of a open contact window and a transistor area was designed as shown in Fig. 8. This configuration produces a linear dependence between the pH ion selective membrane potential and the output voltage. The p–n diode was used from the p^+ ion implant region to n-well. The sensor was built on a silicon wafer (p-type, 100-orientation). The NMOS has 135 Å thickness of the SiO_2 gate and channel to width ratio of 600 μm/20 μm. In the process, the wafers are carried through a standard n-well, LOCOS isolated, polysilicon-gate CMOS process sequence step-by-step. The ISFET uses

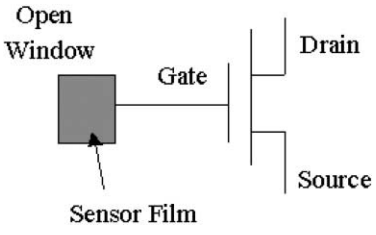

Fig. 8. Schematic diagram of the ISFET.

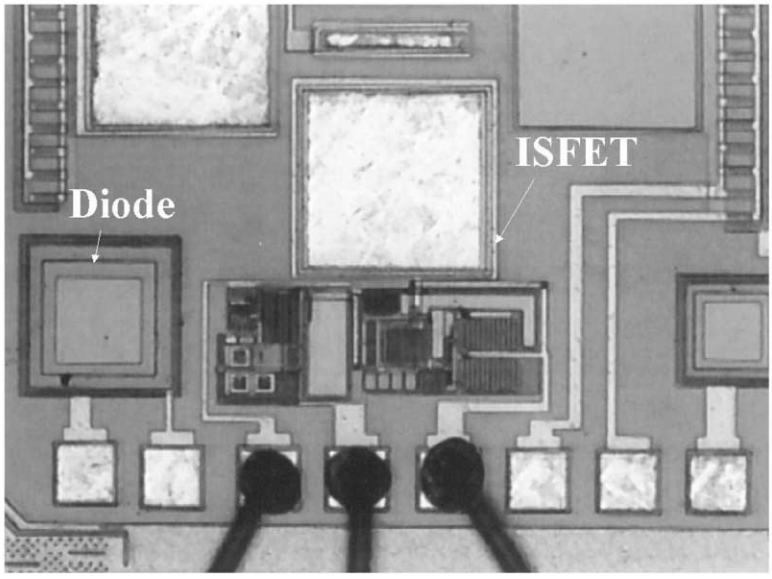

Fig. 9. Layout diagram of the pH-ISFET chip.

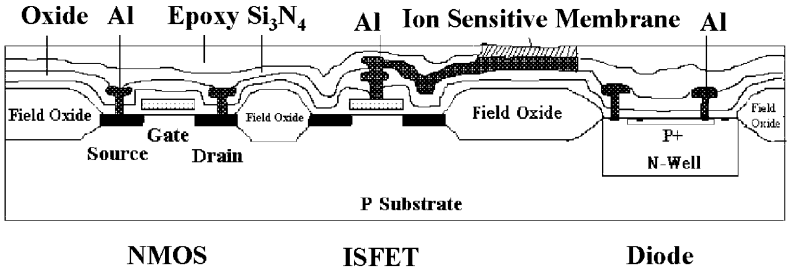

Fig. 10. Cross-section of the discrete gate ISFET and p–n diode.

the NMOS as the base transistor. The mobility is better than that of the PMOS. In the chemically active area, the ion selective membranes were formed on SnO_2/Al multi-layer electrodes in which were connected to the NMOS gate. The chip layout diagram is shown in the Fig. 9 and the cross-section diagram of the ISFET and p–n diode are shown in Fig. 10. An integrated ISFET chip is mounted on a ceramic board and encapsulated with epoxy resin to provide electrical insulation for the bonding wires and exposed silicon regions on the side of the ISFET chip. The epoxy layer was used as a protection layer against ion migration and hydration from the sample solution [22–25].

The SnO_2 thin film was deposited with the self-designed rf sputtering system shown in Fig. 11. The deposition parameters are shown in Table 2 [26–31].

4. Readout circuit

The measuring circuit was completed by feeding both the diode and ISFET output voltages with different gains into a

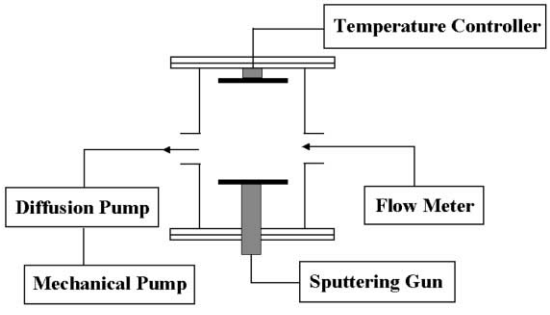

Fig. 11. Schematic diagram of the self-designed rf sputtering system.

Table 2
Growth conditions of film deposition using the sputtering system

Parameters	Conditions
Deposition rate (Å/s)	~20
Deposition pressure (mTorr)	20
Background pressure (Torr)	3×10^{-6}
Ar/O_2 ratio	4:1
Substrate temperature (°C)	150

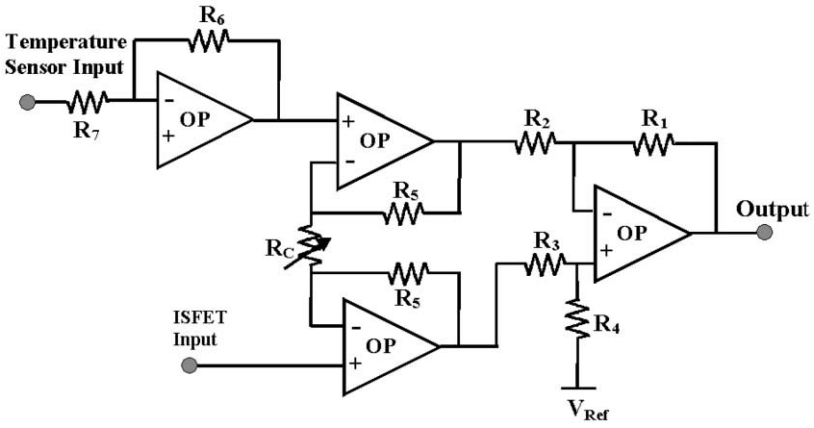

Fig. 12. Schematic diagram of the summation circuit.

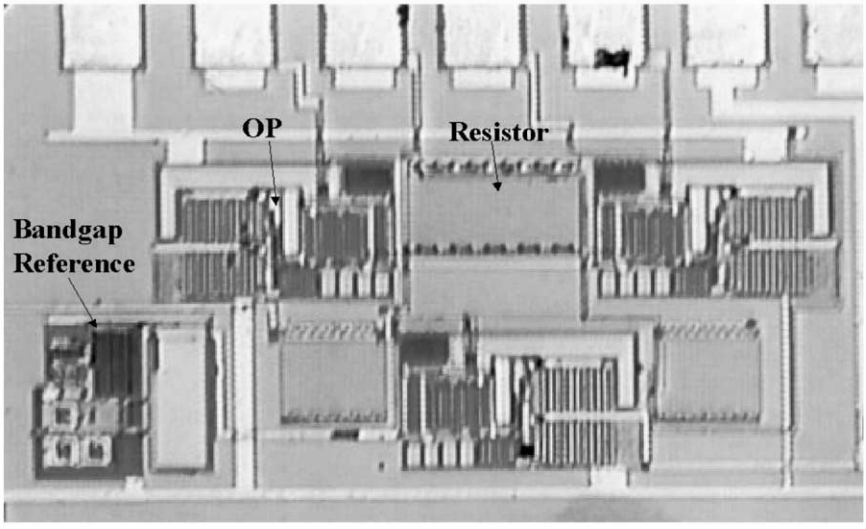

Fig. 13. Layout diagram of the summation circuit.

summing amplifier to mutually offset to their temperature coefficient, and produce a temperature-independent output signal, as shown in Fig. 12. The layout diagram is shown in Fig. 13. The readout circuit for the ISFET is used constant current constant voltage (CCCV) or differential pair with MOSFET and ISFET, shown in the Figs. 14 and 15. Any change in the solution pH affects the solution gate interface potential of the ISFET, which is detected by the ISFET gate as a proportional threshold voltage change. To reduce the temperature effect of bias voltage circuit, a bandgap reference bias circuit was used. The diagram of the circuit is shown in Fig. 16. The diode is operated in forward bias with a constant current. Various temperature, the diode current, which can only be observed as a change in the diode forward voltage since the current is kept constant. The circuit diagram is shown in Fig. 17 [32–36].

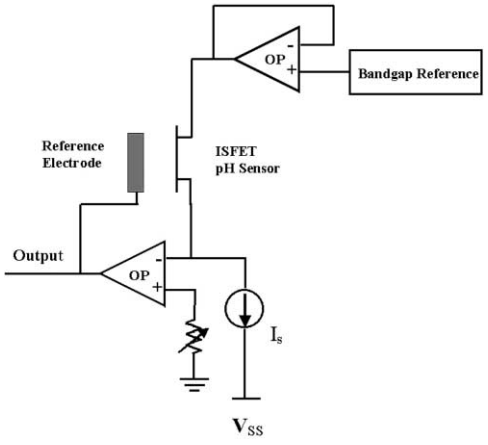

Fig. 14. Block diagram of the constant current constant voltage (CCCV).

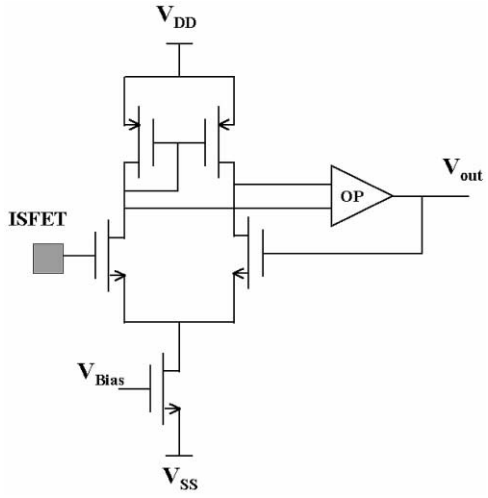

Fig. 15. Schematic diagram of the differential pair with MOSFET and ISFET.

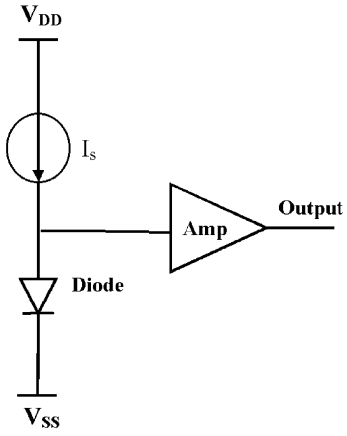

Fig. 17. Schematic diagram of the readout circuit of p–n diode.

5. Results and discussion

5.1. pH sensitivity of the SnO_2/Al discrete gate ISFET

The HP4145B semiconductor parameter analyzer was used to obtain the pH sensitivity of the ISFET in the pH 2, 4, 6, 8, 10 buffer solutions, where the temperature was room temperature (25°C). The ISFET was immersed in a buffer solution for 1 min before testing. The transfer characteristics of an integrated pH-ISFET at various reference voltages (V_{Ref}) and pH buffer solutions are shown in Fig. 18. The reference voltages were applied using an Ag/AgCl reference electrode. The pH sensitivity of the SnO_2/Al gate ISFET can be obtained through a shift in the threshold voltage of an ISFET sensor. The results are as shown in

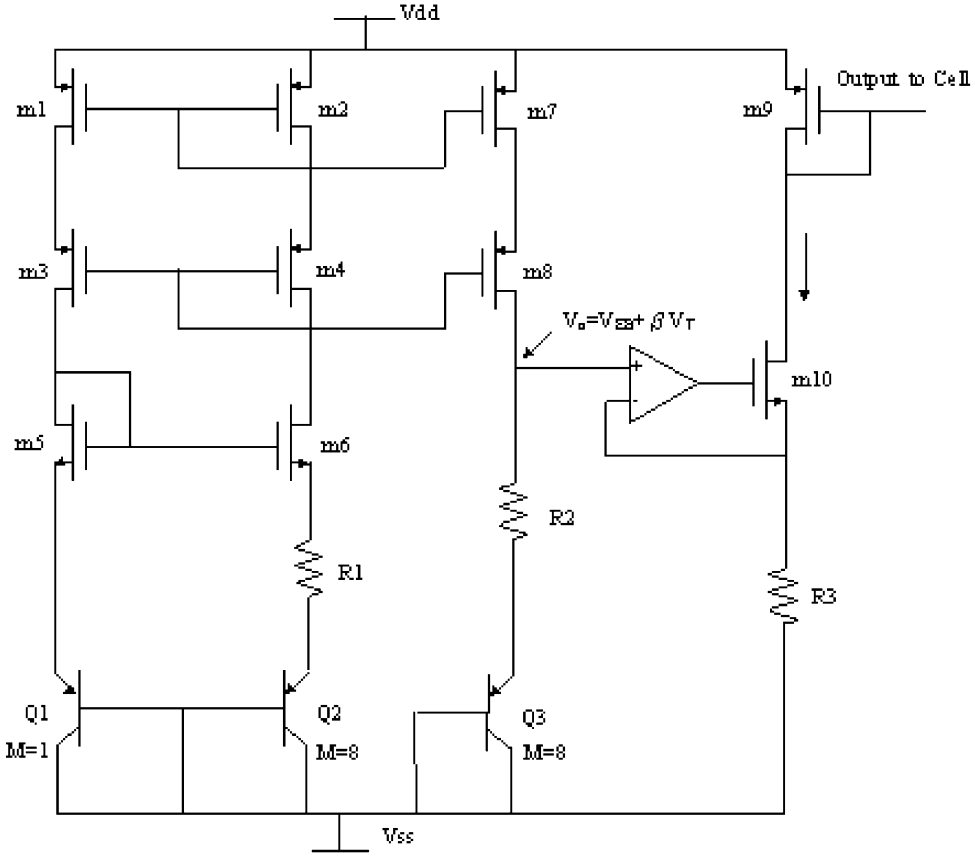

Fig. 16. Schematic diagram of the bandgap reference.

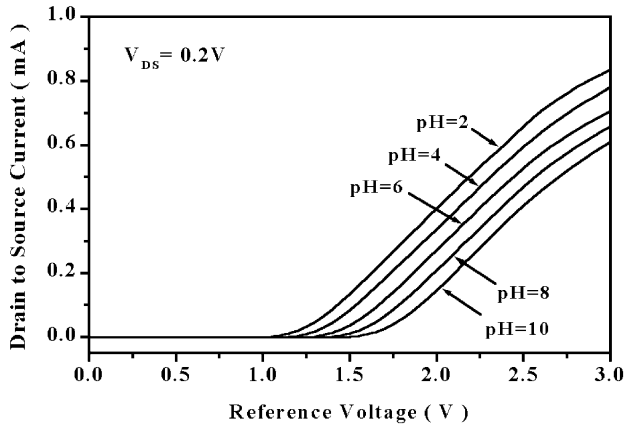

Fig. 18. Curves of the drain-to-source current vs. reference voltage under the different pH buffer solutions.

Fig. 19, in which the SnO_2/Al extended gate ISFET sensor has a linear pH sensitivity of approximately 58 mV per pH in a concentration range between pH 2 and pH 10.

5.2. I–V characteristics of the ISFET device

The ISFET operation is very similar to that of a conventional MOSFET, except that a solution gate was used instead of a metal gate. When the ISFET and a reference electrode (Ag/AgCl) are placed in the pH 2, 4, 6, 8, 10 buffer solutions, a family of curves can be generated by applying 2 V for the voltage of the reference electrode. The I_D–V_{DS} (drain current versus drain-to-source voltage) characteristics of the ISFET in a concentration range between pH 2 and pH 10 are shown in the Fig. 20. The expression for the MOSFET saturation region is as following:

$$I_D = \frac{\mu_n C_{ox}}{2}\frac{W}{L}\left(V_{GS} - \left(E_{Ref} - \Psi_0 + X^{sol} - \frac{\Psi_{Si}}{q} - \frac{Q_{ox}+Q_{ss}}{C_{ox}} - \frac{Q_B}{C_{ox}} + 2\varphi_f\right)\right)^2$$

where μ_n is the mobility of the electrons in the channel ($cm^2\ V^{-1}\ s^{-1}$), C_{ox} the capacitance per unit area of the gate insulator ($pF\ cm^{-2}$), W the channel width (μm), L the channel length (μm), E_{Ref} the contribution of the reference electrode, Ψ_0 the pH-dependent surface potential, X^{sol} the surface dipole potential dipole potential of the solution, Q_{ox} the charges located in the oxide, Q_{ss} the charges located in the surface and interface states, C_{ox} the capacitance due to the oxide film. Based on Eq. (16) and Fig. 20, we have shown that the discrete structure has a linear pH response in the saturation region under the different pH buffer solutions [9].

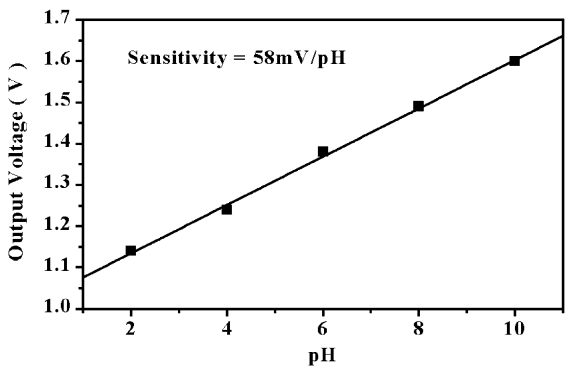

Fig. 19. Curve of the output voltage vs. pH values.

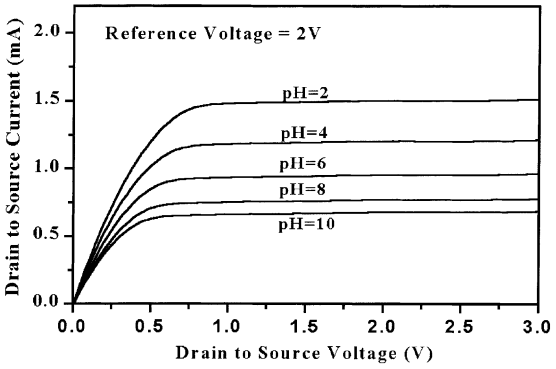

Fig. 20. Curves of the drain-to-source current vs. drain-to-source voltage under the different pH buffer solutions.

5.3. Optical sensitivity of the extended gate ISFET

For conventional MOSFET, the influence of light exposure is negligible, but for open-gate FET-based sensors, optical radiation can cause a considerable threshold voltage shift. The incident light causes a perturbation in the carrier concentrations throughout the semiconductor. In this paper, the extended gate ISFET in which the ion selective membrane was formed on SnO_2/Al multi-layer electrodes. We investigated the optical characteristics of the extended gate ISFET in the dark and under constant light exposure, respectively. We used the constant halogen light exposure of about 2000 lx and illuminated the device of extended gate ISFET, the results are shown in Fig. 21. The data have shown

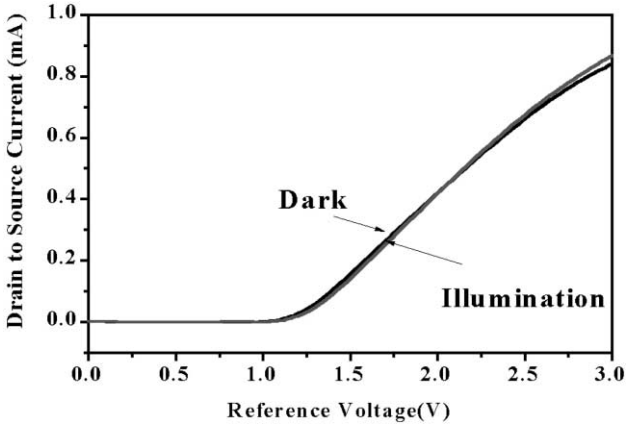

Fig. 21. Optical characteristics of the extended gate ISFET.

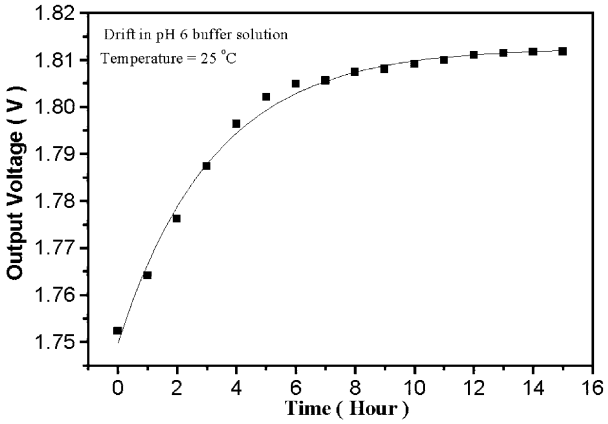

Fig. 22. Drift characteristic of the extended gate ISFET.

that the SnO_2/Al extended gate ISFET structure has an effective decrease in light sensitivity [26,37].

5.4. Drift characteristic of the extended gate ISFET

To study the drift characteristic of the extended gate ISFET. The experimental result described in Fig. 22, which was tested for 15 h. The drift value is 3.96 mV/h [24].

5.5. The temperature characteristics of the p–n diode

For diodes to be reliable temperature sensors, they must display good linearity in order to eliminate tedious calibration. Eq. (17) shows the temperature relationship between the current and voltage of the p–n diode. We measured the current versus voltage at different temperatures as shown in Fig. 23. The parameters of the p–n diode with standard CMOS process are shown in Table 3. Fig. 24 shows good linearity for this diode. They display a fast and stable response for the small change of the temperature.

$$I_D = I_S(e^{qV_D/nKT} - 1) \quad (17)$$

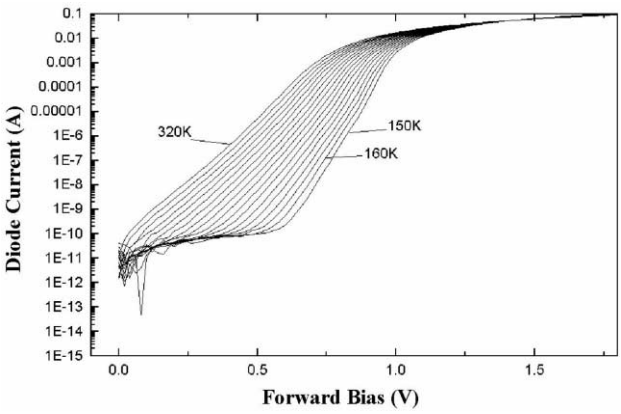

Fig. 23. Curves of the diode current vs. forward bias of p–n diode under different temperature.

Table 3
Parameters of the temperature sensor of the p–n diode with CMOS standard process

	K	I_s (A)	V_T	n
1	200	19.7E−18	0.01725	1.696
2	220	7.51E−16	0.018975	1.66
3	240	9.23E−15	0.0207	1.615
4	260	1.19E−13	0.02425	1.574
5	270	1.05E−13	0.0232375	1.47
6	280	2.62E−13	0.02415	1.44
7	290	6.56E−13	0.025	1.416
8	300	1.92E−12	0.025875	1.410
9	310	5.23E−12	0.0267375	1.41
10	320	1.34E−11	0.0276	1.414

where I_D is the current of the diode, I_S the saturation current, the factor n generally has a value between 1 (for diffusion current) and 2 (for recombination current), V_D the forward voltage of the diode.

Thermal cycle was performed at a constant temperature. The nonlinear temperature coefficient of the solution pH,

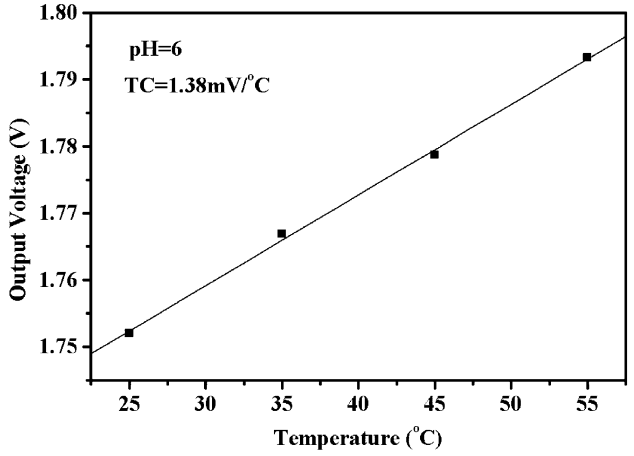

Fig. 25. Curve of the output voltage of ISFET vs. the different temperatures.

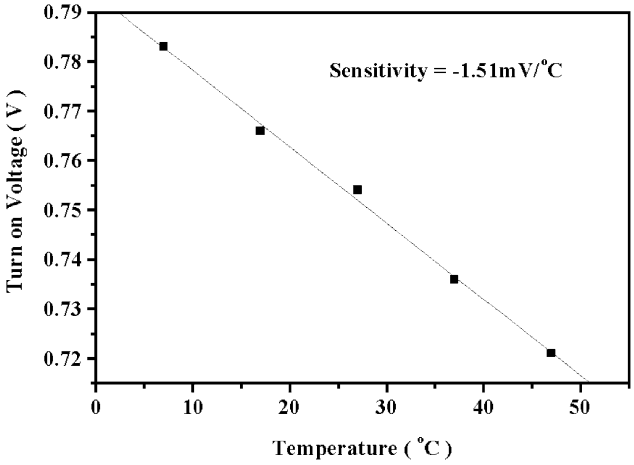

Fig. 24. Sensitivity of the p–n diode with CMOS IC process.

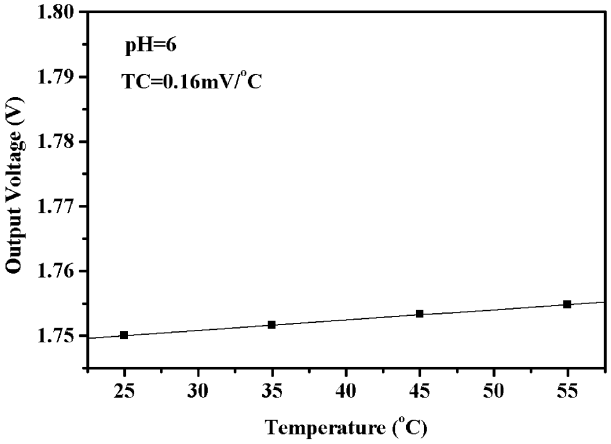

Fig. 26. Curve of the output voltage after temperature compensation.

provided by the manufacturer of the buffer solution, must be taken into account. Using the ISFET's sensitivity (58 mV per pH), the temperature coefficient of +1.38 mV/°C for the ISFET is shown in Fig. 25.

Using the dual sensor design, a marked improvement is shown in pH measurements where the temperature is changed. The output of the temperature compensation circuit is shown in Figs. 12–17. The sensor operated at a drain current of 100 μA in a pH 6 buffer over a temperature range of 25–55°C is shown in Fig. 26. The lower temperature coefficient of 0.16 mV/°C over to wide temperature range shows the distinct advantage of the dual sensor design.

6. Conclusion

We have discussed the ISFET temperature characteristics theory and design of CMOS-integrated ISFET chemical sensor. An integrated ISFET pH sensor system, which consists of the ISFET pH sensor, and a p–n diode temperature sensor, completed with on-chip CMOS amplifiers, was fabricated and evaluated. The temperature coefficient of the ISFET was reduced to 0.16 mV/°C in this device after compensation. The development of integrated sensors and readout circuit may be investigated with all of the advantages of the CMOS IC process. The conclusions can be summarized as follows:

1. Easy CMOS-IC integrated on-chip ISFET processing with the extended gate mode, and the sensitive membranes are the SnO_2/Al.
2. The experimental data show that the SnO_2/Al extended gate ISFET sensor has a linear pH sensitivity of approximately 58 mV per pH in a concentration range between pH 2 and pH 10.
3. The CMOS integrated p–n diode temperature sensor employed sensing and demonstrated compensation to ISFET ambient temperature.
4. The integrated ISFET sensor and p–n diode temperature sensor with on-chip bias and signal conditioning circuits can be produced as a monolithic chip.

Acknowledgements

The authors are indebted to the Chung Shan Institute of Technology for chip bounding wire. Thanks for due to Chip Implementation Center (CIC) for IC product. This work is supported by National Science Council, the Republic of China, under the contract NSC89-2215-E-260-001.

References

[1] P. Bergveld, Develop of an ion-sensitive solid state device for neurophysilogical measurement, IEEE Trans. Biomed. Eng. BME-17 (1970) 70–71.
[2] W. Gui-Hua, Y. Dun, W. Yao-Lin, ISFET temperature characteristics, Sens. Actuators 11 (1987) 221–237.
[3] C.-Y. Aw, P.W. Cheung, A pH-ISFET sensor with on-chip temperature sensing, IEEE Engineering in: Proceedings of the 10th Annual International Conference on Medicine and Biology Society, 1988.
[4] P.R. Barabash, R.S.C. Cobbold, W.B. Wlodarski, Analysis of the threshold voltage and its temperature dependence in electrolyte–insulator–semiconductor field effect transistors (EISFET's), IEEE Trans. Electron Devices ED-34 (6) (1987) 1271–1282.
[5] R.S.C. Cobbold, Transducers for Biomedical Measurements: Principles and Applications, Wiley, New York, 1974.
[6] R. Gomer, G. Tryson, An experimental determination of absolute half-cell EMF's and single ion free energies of solvation, J. Chem. Phys. 66 (1977) 4413–4424.
[7] W.N. Hansen, D.M. Kolb, The work function of immersed electrodes, J. Electroanal. Chem. 100 (1979) 493–500.
[8] L. Bousse, The chemical sensitivity of electrolyte/interface/silicon structures, Ph.D. Dissertation, Twente University of Technology, Enschede, 1982.
[9] H.K. Liao, Study of tin oxide as a sensing film for ISFET applications, Ph.D. Dissertation, Chung Yuan Christian University, Chung Li, 1998.
[10] M. Grattarola, G. Massobrio, S. Martinoia, Modeling H^+-sensitive FET's with SPICE, IEEE Trans. Electron Devices. 39 (4) (1992) 813–819.
[11] H.V.D. Vlekkert, L. Bousse, N. De Roou, The temperature dependence of the surface potential at the Al_2O_3/electrolyte interface, J. Colloid Interf. Sci. 122 (2) (1988) 336–345.
[12] K.I. Tang, Study on Temperature Effect of ISFET Devices, Master Thesis, Hua Fan University, July 1997.
[13] P. Bergveld, The operation of an ISFET as an electronic device, Sens. Actuators Vol. 1 (1981) 17–29.
[14] B.K. Jones, P.C. Russell, Temperature dependence of the MOS mobility degradation, IEEE Proc. 135 (4) (1988) 94–96.
[15] S. Cheng, P. Manos, Effects of operating temperature on electrical parameters in an analog process, IEEE Circuits and Devices Magazine, July 1989, pp. 31–38.
[16] M.-N. Niu, X.-F. Ding, Q.-Y. Tong, Effect of two types of surface sites on the characteristics of Si_3N_4-gate pH-ISFET, Sens. Actuators B 37 (1996) 13–17.
[17] J.-C. Chou, Y.-F. Wang, J.-J. Lin, Temperature effect of a Si:H pH-ISFET, Sens. Actuator B 62 (2000) 92–96.

[18] W. Oelbner, J. Zosel, F. Berthold, H. Kaden, Investigation of the dynamic response behaviour of ISFET pH sensors by means of laser Doppler velocimety (LDV), Sens. Acturators B 26/27 (1995) 345–348.
[19] D. Midgley, Glass pH electrodes with improved temperature characteristics: use of a low-impedance pH sensor as the inner reference electrode, Analyst 115 (10) (1999) 1283–1287.
[20] S. Martinoia, L. Lorenzelli, G. Massobrio, P. Conci, Temperature effects on the ISFET behaviour: simulations and measurements, Sens. Actuators B 50 (1988) 60–68.
[21] T. Katsube, T. Araki, M. Hara, T. Yaji, S. Kobayashi, K. Suzuki, A multi-species biosensor with extended gate field effect transistors, in: Proceedings of the 6th Sensor Symposium, Tokyo, Japan, 1986, pp. 211–214.
[22] H.-S. Wong, M.H. White, A CMOS-integrated "ISFET-operational amplifier" chemical sensor employing differential sensing, IEEE Trans. Electron Devices 36 (3) (1989) 479–487.
[23] K. Dzahini, F. Gaffiot. M. Le Helley, Using a CMOS ASIC technology for the development of an integrated ISFET sensor, In: Proceedings of the International IEEE Euro ASIC'91 Conference, Paris, French, 1991, pp. 356–359.
[24] C. Cane, A. Gotz, A. Merlos, I. Gracia, A. Errachid, P. Losantos, E. Lora-Tamayo, Multi-layer ISFET membranes for microsystems applications, Sens. Actuators B 35/36 (1996) 136–140.
[25] L. Bousse, J. Shott, J.D. Meindl, A process for the combined fabrication of ion sensor and CMOS circuits, IEEE Electron Device Lett. 9 (1) (1988) 44–47.
[26] H.-K. Liao, J.-C. Chou, W.-Y. Chung, T.-P. Sun, S.-K. Hsiung, Study on the interface trap density of the Si_3N_4/SiO_2 gate ISFET, in: Proceedings of the Third East Asian Conference on Chemical Sensors, Seoul, South Korea, 5–6 November 1997, pp. 394–400.
[27] H.-K. Liao, J.-C. Chou, W.-Y. Chung, T.-P. Sun, S.-K. Hsiung, High pH sensitivity of the amorphous tin oxide thin film obtained by thermal vacuum evaporation, in: Proceedings of the 3rd East Asian Conference on Chemical Sensors, Seoul, South Korea, 5–6 November 1997, pp. 410–415.
[28] H.-K. Liao, J.-C. Chou, W.-Y. Chung, T.-P. Sun, S.-K. Hsiung, SnO_2 thin film prepared by rf reactive sputtering for $SnO_2/Si_3N_4/SiO_2$ gate ISFETs applications, in: Proceedings of the First Asia-Pacific International Symposium on The Basic and Application of Plasma Technology, National Yunlin University of Science and Technology, Taiwan, ROC, 15–16 December 1997, pp. 191–194.
[29] H.-K. Liao, J.-C. Chou, W.-Y. Chung, T.-P. Sun, S.-K. Hsiung, Study of amorphous tin oxide thin films for ISFET applications, Sens. Actuators B 50 (1998) 104–109.
[30] L.-L. Chi, Study and fabrication on novel separative structure of enzyme-modified field effect transistor, Master Thesis, 1999.
[31] H.-K. Liao, L.-L. Chi, J.-C. Chou, W.-Y. Chung, T.-P. Sun, S.-K. Hsiung, Study on pH_{PZC} and surface potential of tin oxide gate ISFET, Mater. Chem. Phys. 59 (1999) 6–11.
[32] K. Tsukada, Y. Miyahara, Y. Shibata, H. Miyagi, An integrated micro multi-ion sensor using platinum-gate field effect transistor, In: Proceedings of the International IEEE Transducers'91 Conference, San Francisco, USA, 1991, pp. 218–221.
[33] T.C.W. Yeow, M.R. Haskard, D.E. Mulcahy, H.I. Seo, D.H. Kwon, A very large integrated pH-ISFET sensor array chip compatible with standard CMOS process, Sens. Actuators B 44 (1997) 434–440.
[34] J. Bausells, J. Carrabina, A. Errachid, A. Merlos, Ion-sensitive field effect transistors fabricated in a commercial CMOS technology, Sens. Actuators B 57 (1999) 56–62.
[35] B. Palan, F.V. Santos, J.M. Karam, B. Courtois, M. Husak, New ISFET sensor interface circuit for biomedical applications, Sens. Actuators B 57 (1999) 63–68.
[36] K.F. Sung, The design of a variable gain instrumentation amplifier, Master Thesis, 1999.
[37] C.-L. Wu, J.-C. Chou, W.-Y. Chung, T.-P. Sun, S.-K. Hsiung, Study on $SnO_2/Al/SiO_2/Si$ ISFET with a metal light shield, Mater. Chem. Phys. 63 (2000) 153–156.

Biographies

Yuan-Lung Chin was born in Taiwan, ROC, in 1963. He received the BS degree in electrical engineering from Chung Yung University of Taiwan, ROC, in 1990 and the MS degree in electrical engineering from Chung Yung University in 1996. He is current working toward the PhD degree in the Department of Electrical Engineering at Chung Yung University. His research topics include the characterization of metal oxide materials and applications for ISFET sensors and analog/digital mixed-mode integrate circuit design.

Jung-Chuan Chou PhD, was born in Tainan, Taiwan, ROC, on 13 July 1954. He received the BS degree in physics from Kaohisung Normal College, Kaohsiung, Taiwan, ROC, in 1976; the MS degree in applied physics from Chung Yuan Christian University, Chung-Li, Taiwan, ROC, in 1979; and the PhD degree in electronics from National Chiao Tung University, Hsinchu, Taiwan, ROC, in 1988. He taught at Chung Yuan Christian University from 1979 to 1991. Since 1991 he has worked as an associate professor in the Department of Electronic Engineering at the National Youlin University of Science and Technology. His research interests are in the areas of amorphous materials and devices, electrographic photoreceptor materials and devices, electronic materials and devices, sensor devices, and science education.

Tai-Ping Sun was born in Taiwan, ROC, on 20 March 1950. He received the BS degree in electrical engineering from Chung Cheng Institute of Technology, Taiwan, ROC, in 1974, the MS degree in material science engineering from National Tsing Hua University, Taiwan, ROC, in 1977, and PhD degree in electrical engineering from National Taiwan University, Taiwan, ROC, in 1990. From 1977 to 1997, he worked at Institute of Science and Technology, Taiwan, ROC, concerning the development of infrared device, circuit and system. Since 1999 he has joined the Department of Electrical Engineering, National Chi Nan University as a professor and his research interests are in infrared detector and system, analog/digital mixed-mode integrated circuit design, special semiconductor sensor and their application.

Wen-Yaw Chung was born in Hsin-Chu, Taiwan, ROC, on 15 March 1957. He received the BSEE and MS degrees from Chung Yuan Christian University, Chung Li, Taiwan, ROC, in 1979 and 1981, respectively, and the PhD degree in Electrical and Computer Engineering from Mississippi State University, USA, in 1989. Subsequently, he joined the Advanced Microelectronics Division, Institute for Technology Development in Mississippi, where he was involved in the design of a bipolar optical data receiver. In CMOS data communication integrated circuits. Since 1991 he has been an Associate Professor in the Department of Electronic Engineering at Chung Yuan Christian University. His research interests include mixed-signal VLSI design, biomedical IC applications, and test-chip design methodology for deep submicron VLSI electronics.

Shen-Kan Hsiung was born on 14 June 1942. He received the BS degree from Department of Electrical Engineering, National Cheng-Kung University, in 1965, the MS degree from Department of Electronic Engineering, National Chiao-Tung University, Taiwan, ROC, in 1968 and the PhD degree from Material Science Engineering of USC, USA in 1974. From 1974 to 1978, he was an associate professor in Department of Electrical Engineering, Chung Yuan Christian University. Since 1978 he has been a professor in Department of Electronic Engineering, Chung Yuan Christian University. His current interests are electronic materials, amorphous thin films and semiconductor sensors.